Exhibit C

THE JOURNAL OF BIOLOGICAL CHEMISTRY
Vol. 277, No. 1, Issue of January 4, pp. 155–160, 2002
Printed in U.S.A.

Proteolytic Sensitivity and Helper T-cell Epitope Immunodominance Associated with the Mobile Loop in Hsp10s*

Received for publication, August 9, 2001, and in revised form, October 9, 2001
Published, JBC Papers in Press, October 22, 2001, DOI 10.1074/jbc.M107624200

Stephanie Carmicle, Guixiang Dai, N. Kalaya Steede, and Samuel J. Landry‡

From the Department of Biochemistry, Tulane University Health Sciences Center, New Orleans, Louisiana 70112-2699

Antigen three-dimensional structure potentially limits antigen processing and presentation to helper T-cell epitopes. The association of helper T-cell epitopes with the mobile loop in Hsp10s from mycobacteria and bacteriophage T4 suggests that the mobile loop facilitates proteolytic processing and presentation of adjacent sequences. Sites of initial proteolytic cleavage were mapped in divergent Hsp10s after treatment with a variety of proteases including cathepsin S. Each protease preferentially cleaved the Hsp10s in the mobile loop. Flexibility in the 22-residue mobile loop most probably allows it to conform to protease active sites. Three variants of the bacteriophage T4 Hsp10 were constructed with deletions in the mobile loop to test the hypothesis that shorter loops would be less sensitive to proteolysis. The two largest deletions effectively inhibited proteolysis by several proteases. Circular dichroism spectra and chemical cross-linking of the deletion variants indicate that the secondary and quaternary structures of the variants are native-like, and all three variants were more thermostable than the wild-type Hsp10. Local structural flexibility appears to be a general requirement for proteolytic sensitivity, and thus, it could be an important factor in antigen processing and helper T-cell epitope immunogenicity.

Numerous studies indicate that the context of a T-helper epitope influences its immunogenicity (1–6). Cryptic epitopes can be shielded from presentation by various mechanisms that ultimately interfere with binding of peptides to the class II MHC[1] protein (7) or transport of the complex to the cell surface (8). Antigen processing contributes directly to these mechanisms by removing or failing to remove antigen sequences that influence presentation of the epitope. Studies testing the role of proteases in knock-out mice have been complicated by the requirement for proteolytic maturation of the class II MHC protein. Nevertheless, antigen presentation is altered when cathepsin S or cathepsin L deficiency is combined with invariant chain deficiency (9). Thus, the pathway of proteolytic degradation can influence antigen presentation.

Early studies suggested that antigen primary sequence affected antigen processing at the level of recognition and binding by a protease (1, 10). More recently, the effect of cleavage site primary sequence on immunogenicity was demonstrated. The creation of a dibasic cleavage site for a prohormone processing enzyme enhanced the presentation of a flanking epitope in hen egg lysozyme (11), and disruption of a cleavage site for asparaginyl endopeptidase interfered with presentation of the tetanus toxoid antigen (12).

However, other reports have suggested that three-dimensional structure modulates antigen processing. Stabilization by intramolecular cross-links inhibited presentation of an epitope of hen egg lysozyme (13). An acid-induced structural change enhanced presentation of an epitope of influenza hemagglutinin (3). Unfolding prior to processing disrupted presentation of an immunodominant epitope of mouse immunoglobulin (2).

The distribution of local disorder in the antigen could modulate antigen processing. It is well established that proteases tend to cleave between domains in multi-domain proteins and at other locally disordered sites. Even in a single-domain protein, proteolytically sensitive sites tend to occur in segments characterized by high crystallographic B-factors (14). The conformation of the polypeptide around the incipient cleavage site must be easily distorted to accommodate binding to the protease (15, 16). To our knowledge, no ATP-dependent protein unfolding activity (other than acidification) has been described for the lysosome. The pH of the antigen-processing compartment probably depends on the cell type and degree of activation (17). Nevertheless, most proteins retain native-like three-dimensional structure in acidic environments as low as pH 2 in many cases (18).

Analyses of published structural data and epitope maps for several model antigens have suggested that local structural disorder increases immunogenicity in the adjacent sequences (19, 20). Here, we have tested this hypothesis by analyzing the structure and immunology of bacteriophage T4 Hsp10 (T4Hsp10). As in all Hsp10s, T4Hsp10 has a flexibly disordered Hsp60-binding mobile loop (21) that we suspected would favor presentation of flanking sequences to helper T-cells. T4Hsp10 is homologous to bacterial and mammalian Hsp10s by comparison of the respective three-dimensional structures, although it exhibits less than 20% sequence identity with any of these Hsp10s (22). The mobile loops of *Escherichia coli* Hsp10 (GroES) and T4Hsp10 contain preferred sites for cleavage by trypsin and protease K, respectively (20, 23). Earlier studies have mapped helper T-cell epitopes to sequences flanking the mobile loop of *Mycobacterium leprae* Hsp10 in infected humans and immunized mice (24–26). In a companion paper (27), we confirm the presence of an immunodominant epitope adjacent to the mobile loop in T4Hsp10.

Here, we examined the potential for three-dimensional structure to influence processing and presentation by analyzing the proteolytic sensitivity of the mobile loop in Hsp10s. We find that treatment of diverse Hsp10s with a variety of proteases

* This work was supported by National Institutes of Health Grant R01-AI42350. The costs of publication of this article were defrayed in part by the payment of page charges. This article must therefore be hereby marked "*advertisement*" in accordance with 18 U.S.C. Section 1734 solely to indicate this fact.

‡ To whom correspondence should be addressed: Dept. of Biochemistry, Tulane University Health Sciences Center, 1430 Tulane Ave., New Orleans, LA 70112-2699. Tel.: 504-586-3990; Fax: 504-584-2739; E-mail: landry@tulane.edu.

[1] The abbreviations used are: MHC, major histocompatibility complex; Hsp, heat shock protein; T4Hsp10, bacteriophage T4 Hsp10; MES, 4-morpholineethanesulfonic acid; E-64, trans-epoxysuccinyl-L-leucylamido-(4-guanidino)butane.

TABLE I
Products of Hsp10 limited proteolysis assigned by mass spectrometry

Hsp10	Protease	N-terminal fragment				C-terminal fragment			
		Observed	Predicted	Difference	Sequence	Observed	Predicted	Difference	Sequence
			Da				*Da*		
E. coli	Cathepsin S	3158	3159	−1	Met^{1}–Thr^{28}	7225	7241	−16	Glu^{29}–Ala^{97}
	Papain	3060	3059	1	Met^{1}–Leu^{27}	7345	7342	3	Thr^{28}–Ala^{97}
Human	Cathepsin S	3048	3050	−2	Ala^{1}–Lys^{27}	7754	7764	−10	Gly^{28}–Asp^{101}
		3406	3408	−2	Ala^{1}–Met^{31}	7402	7406	−4	Leu^{32}–Asp^{101}
	Papain	3062	3050	12	Ala^{1}–Lys^{27}	7785	7764	21	Gly^{28}–Asp^{101}
		2934	2922	12	Ala^{1}–Thr^{26}	7908	7892	16	Lys^{27}–Asp^{101}
		3419	3410	9	Ala^{1}–Met^{31}	7429	7411	18	Leu^{32}–Asp^{101}
	Proteinase K	3048	3050	−2	Ala^{1}–Lys^{27}	7765	7764	1	Gly^{28}–Asp^{101}
		3405	3408	−3	Ala^{1}–Met^{31}	7410	7406	4	Leu^{32}–Asp^{101}
		3744	3747	−3	Ala^{1}–Glu^{34}	7085	7067	18	Lys^{35}–Asp^{101}

consistently yields products of initial cleavage in the mobile loop, suggesting that antigen processing by lysosomal proteases would initiate with cleavage in the mobile loop. Variants of T4Hsp10 containing deletions in the mobile loop were constructed in order to probe the changes in protease sensitivity and immune responses. Our results suggest that loop deletion can reduce proteolytic sensitivity without gross disruption of antigen three-dimensional structure. In a companion paper (27) we show that reduced proteolytic sensitivity correlates with reduced helper T-cell and antibody epitope immunodominance.

MATERIALS AND METHODS

Proteins and Peptides—Deletions in the T4Hsp10 coding sequence of plasmid pAlex (a kind gift of A. Richardson, University of Geneva, Switzerland) were introduced using the Stratagene site-directed mutagenesis kit. DNA sequencing confirmed the native sequence of each construct, with the exception of the intended mutation. Protein purification was executed as previously described for T4Hsp10 (28), except that the Superdex-200 gel-filtration step was substituted with hydroxyapatite chromatography employing a 20–300 mM gradient of sodium phosphate, pH 6.8.

Limited Proteolysis—All reactions were carried out in a total volume of 50 μl and contained 100 μM T4Hsp10, T4Hsp10dLIG, T4Hsp10d8, or T4Hsp10d8C (subunits) except where otherwise noted. All enzymes were from Sigma and of the highest grade available. Reactions with trypsin containing 10 mM Tris-HCl, pH 7.5, and 5 μg/ml protease proceeded for 30 min on ice and then were terminated by the addition of phenylmethylsulfonyl fluoride to 20 μM. Reactions with protease V8 containing 50 mM sodium phosphate, pH 7.5, 1 μM dithiothreitol, and 25 μg/ml protease proceeded for 30 min at room temperature and then were terminated by the addition of Nonidet P-40 to 1.5%. Reactions with cathepsin S (kind gift of M. McGrath, Axys Pharmaceuticals, Inc.) in a total volume of 65 μl containing 50 mM Tris-HCL, pH 7.5, 192 mM KCl, 1 μM dithiothreitol, and 0.8 μg/ml protease proceeded for 30 min at room temperature and then were terminated by the addition of E-64 (Sigma) to 10 μM. Reactions with protease K containing 50 μM target protein, 40 mM Tris-HCl, pH 7.5, 192 mM KCl, 1 μM dithiothreitol, and 25 μg/ml protease proceeded for 15 min on ice and then were terminated by the addition of phenylmethylsulfonyl fluoride to 20 μM. Reactions with papain containing 10 mM MES-KOH (pH 5.7), 4 mM β-mercaptoethanol, and 20 μg/ml protease proceeded for 60 min at room temperature and then were terminated by the addition of E-64 to 5 μM. An aliquot of each reaction was mixed with SDS-containing sample buffer, resolved by SDS-PAGE using the Tris/Tricine buffer system (29), and stained with Coomassie Blue. Quantification of the remaining intact protein was by integration of the band in the image of the stained gel captured by an AlphaImager 2200 (Alpha Innotech).

Mass Spectrometry—For mapping cleavage sites in *E. coli* and human Hsp10s, 0.5 μl of the reaction was analyzed using a Thermofinnigan Lasermat matrix-assisted laser desorption time-of-flight (MALDI-TOF) mass spectrometer (Tulane Coordinated Instrumentation Facility) and α-cyano-3-hydroxycinnamic acid as the matrix. Mass determinations were calibrated with substance P ($(M + H)^+$, 1349 Da), which was co-deposited on the target prior to analysis. Fragment mass predictions were generated with PeptideMass[2] using Swiss-Prot sequence entries CH10ECOLI or CH10HUMAN.

[2] Found on the Internet at www.expasy.ch.

Circular Dichroism Spectroscopy—Far-UV circular dichroism (CD) spectra were recorded on an OLIS spectropolarimeter using a cell with path length 1 mm. Samples contained 25 μM protein (subunits) in 10 mM sodium phosphate, pH 6.8, at 25 °C. The wavelength was scanned in triplicate between 300 and 188.2 nm using 110 points, and the spectra were averaged. A similarly recorded background spectrum was subtracted from the sample spectrum to obtain the protein spectrum. Melting curves monitored by CD were obtained by recording the CD at 205 and 206 nm at 2° intervals over the range of 22 to 84 °C and then averaging the values at the two wavelengths for each temperature (reported as $\theta_{205.5}$). The data for each protein were fit by nonlinear regression (GraphPad Prism) to the equation

$$y = \{(y_f + m_f \cdot [T]) + (y_u + m_u \cdot [T]) \cdot \exp[(\Delta H_m/RT) \cdot ((T - T_m)/T_m)]\}/(1 + \exp[(\Delta H_m/RT) \cdot ((T - T_m)/T_m)]) \quad \text{(Eq. 1)}$$

where y represents the observed CD signal, y_f and y_u are the intercepts, and m_f and m_u the slopes of the pre- and posttransition base lines, T is the temperature, T_m is the midpoint of the thermal unfolding curve, and ΔH_m is the enthalpy change for unfolding at T_m (30). Thermal unfolding was found not to be reversible, and thus ΔH_m cannot be taken as the enthalpy for equilibrium unfolding of the protein. Nevertheless, T_m gives an indication of protein stability against thermal denaturation.

Glutaraldehyde Cross-linking—Reactions were initiated by addition of 25% glutaraldehyde to achieve a final concentration of 2% (w/v) in 100 μl of 5 mM sodium phosphate buffer, pH 6.8, and 100 μM T4Hsp10, T4Hsp10dLIG, T4Hsp10d8, or T4Hsp10d8C. After 2, 10, or 20 min at room temperature, reactions were quenched by the addition of sodium borohydride to a final concentration of 400 mM. After 20 min, proteins were precipitated at room temperature with 10% trichloroacetic acid in the presence of 100 mM NaCl, collected by centrifugation at 15,000 × *g*, combined with NuPAGE LDS sample buffer (Invitrogen), run on a NuPAGE bis-Tris 4–20% polyacrylamide gel with NuPAGE MES buffer (Invitrogen), and stained with Coomassie Blue.

RESULTS

Preferred Cleavage Sites in the Mobile Loop

The proteolytic sensitivity of diverse Hsp10 proteins was probed with several serine and cysteine proteases including cathepsin S. Cysteine proteases constitute the bulk of the lysosomal proteases, and cathepsin S has been implicated in antigen processing (9). A strong preference for cleavage in the mobile loop should dominate the cleavage site selectivity regardless of Hsp10 sequence or protease specificity. Such a highly preferred site most likely would be the site of first cleavage by the mixture of proteases in the lysosome. For each combination of Hsp10 and protease, experimental conditions were optimized for the accumulation of products resulting from an initial endoproteolytic cleavage, as judged by the resolution of one or more large fragments in SDS-PAGE.

For each protease and Hsp10, one or more abundant fragments were observed at ~3000 and 7000 Da by mass spectrometry (Table I). Cleavage sites (Fig. 1) were identified by the presence of both N- and C-terminal fragments corresponding to

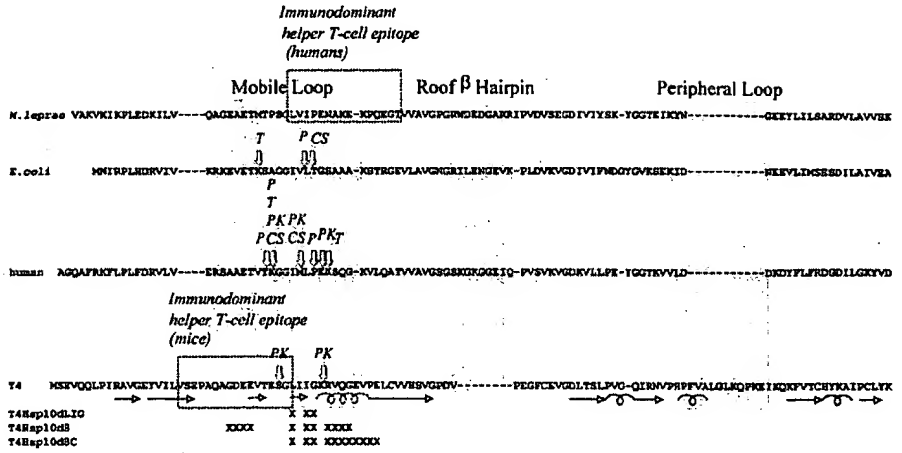

FIG. 1. **Alignment of Hsp10 sequences indicating structural features and preferred sites for endoproteolytic cleavage (*T*, trypsin; *P*, papain; *CS*, cathepsin S; *PK*, protease K).** The immunodominant helper T-cell epitopes of *M. leprae* Hsp10 in humans and of T4Hsp10 in mice are from Refs. 24 and 27, respectively. Locations of β-strands (*arrows*) and α or 3_{10} helices (coils) are indicated *below* the sequence of T4Hsp10. Nascent elements of secondary structure are indicated with *dashed lines*. Residues deleted in the T4Hsp10 variants are indicated with "*X*". Data for trypsin cleavage of *E. coli* Hsp10 and protease K digestion of T4 Hsp10 were from Refs. 23 and 21, respectively.

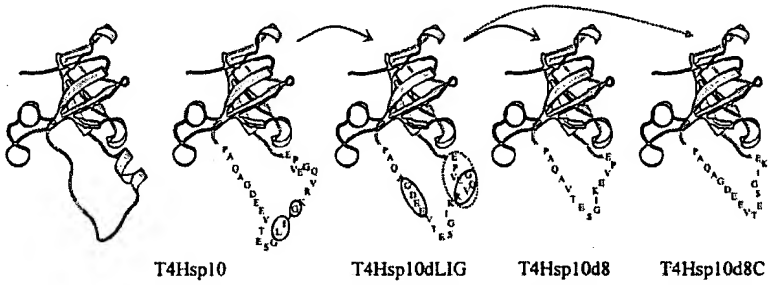

FIG. 2. **Ribbon diagrams of a single subunit of T4Hsp10 indicating residues deleted in the mobile loop deletion variants.** The mobile loop (Gln^{24}–Val^{45}) plus two residues on each flank are indicated in single-letter code. In the construction of T4Hsp10dLIG, the removal of Leu^{35} and Ile^{36} (*circled*) repositions Ile^{37} opposite Thr^{31} in the nascent hairpin, which can provide a stabilizing interaction (31); and removal of Gly^{38} (*circled*) reduces flexibility. In the construction of T4Hsp10d8, four residues (*circled*) are deleted from each flank of the nascent hairpin in T4Hsp10dLIG. In the construction of T4Hsp10d8C, eight residues (*broken circle*) are deleted from the C-terminal flank of the nascent hairpin in T4Hsp10dLIG. T4Hsp10d8C lacks the entire segment comprising a small helix that was stabilized by the crystal lattice (22).

the masses predicted from the Hsp10 sequence (±21 Da). There were several examples of alternative cleavage sites in human Hsp10 for a single protease. A secondary site was evident as a less abundant pair of large and small fragments. It was clear that each fragment was derived from cleavage of the full-length protein for the following two reasons. First, the difference in mass between large fragments was equal to the difference in mass between small fragments; and second, the difference was equal to the mass of residues between the alternative sites, *e.g.* Gly^{28}–Met^{31} in the cathepsin S digestion of human Hsp10. Initial cleavage sites in T4Hsp10 could not be determined from the mass spectrometry data. Although fragments clustered near 3000 and 7000, the sum of the masses for predominant fragments was less than the total mass of T4Hsp10. Presumably, the initial cleavage products were rapidly converted to smaller fragments.

Deletions in the Mobile Loop Stabilize T4Hsp10 and Inhibit Proteolysis

Deletion Design—Deletion variants of T4Hsp10 were constructed to test the relationship of mobile loop size and flexibility to proteolytic sensitivity (Fig. 2). We reasoned that a shorter loop would have less flexibility to adopt the conformation necessary for binding to a protease. The 3-residue deletion in T4Hsp10dLIG was designed to shorten the loop and stabilize a nascent hairpin turn in the center of the loop (21) by removing a glycine and by placing an isoleucine opposite threonine 31 on the other β-strand (31). The 8-residue deletion in T4Hsp10d8 symmetrically removed from T4Hsp10dLIG four residues in each strand of the nascent hairpin. The 8-residue deletion in T4Hsp10d8C removed from T4Hsp10dLIG a segment that forms an α helix in the T4Hsp10 crystal lattice but that is essentially disordered in solution (21). The deletions affect sequences only within the mobile loop and thus were not expected to disturb the ordered part of the native structure.

Purification and Secondary Structure—The biophysical properties of the deletion variants were similar to those of wild-type T4Hsp10. Each variant accumulated in the soluble phase of *E. coli* cells at high levels and was purified using the protocol developed for T4Hsp10. T4Hsp10 and the three variants eluted from Q-Sepharose at the same position in the gradient, but the variants eluted from hydroxyapatite at elevated sodium phosphate concentrations. Whereas T4Hsp10 eluted at 65 mM, T4Hsp10dLIG eluted at 70 mM, T4Hsp10d8 at 120 mM, and T4Hsp10d8C at 150 mM. The far-UV CD spectra of T4Hsp10 and the deletion variants were similar, as expected for retention of the native, mostly β-sheet secondary structure (Fig. 3*A*). However, in the spectrum of T4Hsp10d8C, the intensity of the band at 198 nm was more positive, which is consistent with a larger fraction of β-sheet (32).

Thermal Stability—The thermal stability of T4Hsp10 and the deletion variants was evaluated by monitoring the CD at 205.5 nm over the temperature range of 22 to 84 °C. Thermal denaturation of all four proteins was evident as a cooperative transition in the CD intensity (Fig. 3*B*). Spectra recorded after the transition exhibited strong minima near 200 nm (data not shown), which is expected if a substantial portion of the denatured proteins behaves as a random coil (32). The deletion variants melted at temperatures ranging from 3 to 7 °C higher than T4Hsp10.

Cross-linking with Glutaraldehyde—The quaternary structures of T4Hsp10 and the deletion variants were analyzed by

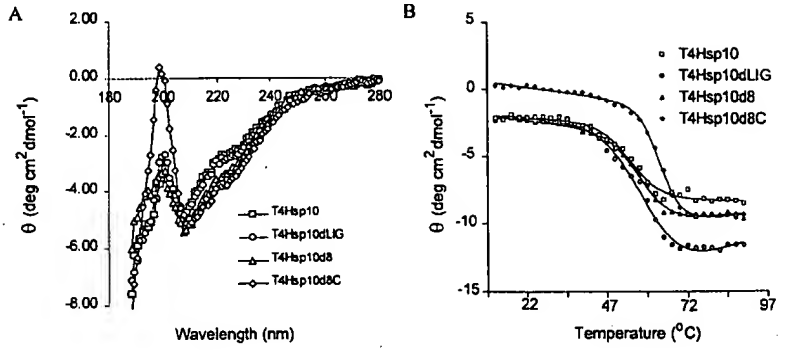

FIG. 3. **CD spectra (*A*) and thermal denaturation curves (*B*) for T4Hsp10 and mobile loop deletion variants.** The similar spectra indicate similar secondary structure content in the four proteins, although the more positive band at 198 nm reports a slightly larger β-sheet content for T4Hsp10d8C. For all four proteins, heat denaturation monitored by CD at 205.5 nm exhibits a cooperative transition. All three variants are more thermostable than T4Hsp10. The T_m values were as follows (in °C): T4Hsp10, 56.0; T4Hsp10dLIG, 59.5; T4Hsp10d8, 58.5; and T4Hsp10d8C, 63.3.

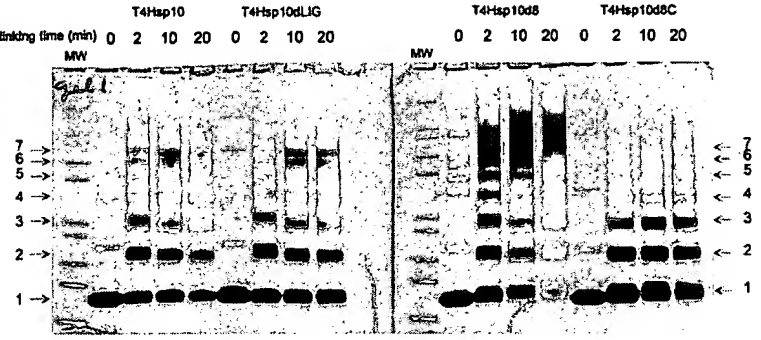

FIG. 4. **Oligomeric structure of T4Hsp10 and mobile loop deletion variants.** Treatment of T4Hsp10 with glutaraldehyde produced a ladder of six cross-linked species corresponding to dimer through heptamer (identified by *arrows* labeled *2–7*). Increasing the time of incubation with cross-linker increased the amount of heptamer and decreased the amount of smaller species but did not result in the formation of discrete species larger than a heptamer.

chemical cross-linking. Treatment of T4Hsp10 with glutaraldehyde generated a ladder of six polypeptides with slower electrophoretic mobility in SDS-PAGE (Fig. 4). Because T4Hsp10 is known to form a heptamer (22), we assigned the six bands to dimer through heptamer. The bands were less intense with increasing molecular weights up to hexamer and heptamer, which were more intense than pentamer. A longer incubation with the cross-linker increased the intensity of the hexamer and heptamer at the expense of lower molecular weight bands, but no discrete bands above heptamer were formed. Thus, we concluded that the cross-linking reaction with T4Hsp10 is essentially complete upon formation of the heptamer.

Each deletion variant formed a ladder of cross-linked polypeptides that was similar to that formed by T4Hsp10. As for T4Hsp10, a longer incubation with the cross-linker increased the amount of heptamer but not higher order multimers. The cross-linked samples of T4Hsp10d8 also produced a diffuse band near and above the molecular weight of heptamer. This material probably is the result of multiple intersubunit and/or intrasubunit cross-links (33, 34), which are somehow more likely in the modified mobile loop. Nevertheless, among the discrete cross-linked species after the 10-min incubation, the heptamer was the most abundant. The heptamer species of T4Hsp10d8C was poorly represented among the cross-linked species. This variant may have been resistant to cross-linking because the mobile loop was less flexible. At longer incubation times, more of the T4Hsp10d8C accumulated in the tetramer and pentamer forms, suggesting that an oligomer of that size or larger predominated. Because the cross-linked species discontinued above the level of heptamer, we concluded that T4Hsp10d8C also existed predominantly as the heptamer.

Limited Proteolysis—Differences between T4Hsp10 and the deletion variants in proteolytic sensitivity were largely independent of the choice of protease (Fig. 5). Sensitivity of T4Hsp10dLIG was similar to that of T4Hsp10 except for slight decreases in sensitivity to trypsin (30%) and protease V8 (20%). T4Hsp10d8 was much less sensitive than T4Hsp10 to trypsin (6-fold) and cathepsin S (6-fold) but only slightly less sensitive to protease K (10%) and protease V8 (20%). T4Hsp10d8C was much less sensitive than T4Hsp10 to all four proteases (protease K, 4-fold; trypsin, 5-fold; protease V8, 36-fold; and cathepsin S, 14-fold).

DISCUSSION

Earlier work comparing helper T-cell epitope maps to structural data indicated that helper T-cell epitopes were frequently associated with adjacent unstable loops. We hypothesized that unstable loops promote presentation of adjacent sequences by virtue of their sensitivity to endoproteolytic processing in antigen presenting cells. For the present work, Hsp10 was selected for an examination of the relationship of structure and proteolytic sensitivity because helper T-cell epitopes have been found adjacent to the mobile loop (24–27), and the mobile loop provides a natural target for initial endoproteolytic cleavage during antigen processing.

Results from mapping the sites of initial cleavage in *E. coli* and human Hsp10s demonstrate the exceptional proteolytic sensitivity of the mobile loop. When combined with the earlier studies on *E. coli* and bacteriophage T4 Hsp10s, we find that four proteases cleave three divergent Hsp10s within a 12-residue segment of the 22-residue mobile loop. The shared preference of the proteases for this segment cannot be attributed to a coincidence of required primary sequences. The proteases exhibit little sequence specificity (35). Trypsin requires a positively charged residue (Lys/Arg) in P1, but the 13 Lys/Arg in *E. coli* Hsp10 and the 15 Lys/Arg in human Hsp10 are evenly distributed in the sequences. The other proteases are less specific. Proteinase K prefers aromatic and hydrophobic residues in P1. Papain prefers bulky hydrophobic residues in P2 and slightly prefers Lys/Arg in P1. Cathepsin S prefers branched hydrophobic residues in P2. Local structural disorder in the mobile loop probably is the most important factor determining the initial cleavage site. Local disorder is typical of protein segments that are easily distorted into a conformation suitable for binding to the protease active site (15).

Preferential cleavage in the mobile loop can be explained by the loop being larger and more flexible than other potentially protease-sensitive sites in the Hsp10s (Fig. 6). The roof β-hair-

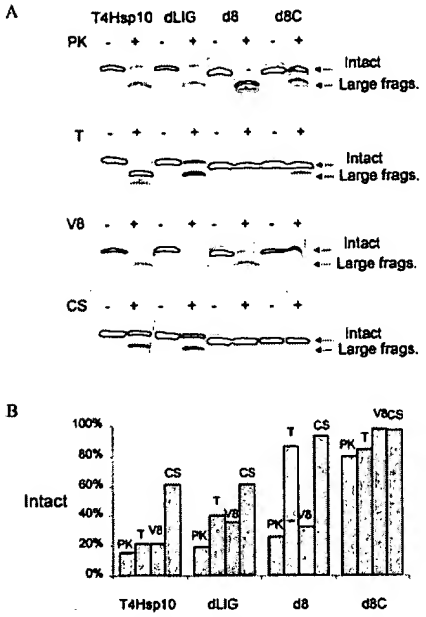

FIG. 5. **Proteolytic sensitivity of T4Hsp10 and mobile loop deletion variants.** *A*, reaction conditions with T4Hsp10 were optimized for accumulation of large fragments (*Large frags.*) detected by SDS-PAGE, and then the same conditions were employed with the deletion variants. *B*, quantification of intact protein following limited proteolysis. Proteases designations are the same as in the legend for Fig. 1; *V8*, protease V8. T4Hsp10 variants are designated by the suffix identifying the deletion (*dLIG* for T4Hsp10dLIG, etc.). Proteolytic sensitivity was defined in terms of the fraction degraded in the illustrated reactions. The fraction degraded was taken as the fraction intact subtracted from unity. The intact fraction was measured as the integrated intensity of the intact band in the treated lane divided by the integrated intensity of the intact band in the mock-treated control lane. T4Hsp10dLIG was only slightly less sensitive than T4Hsp10 to trypsin and protease V8. In contrast, T4Hsp10d8 was six times less sensitive to trypsin, and cathepsin S. T4Hsp10d8C was at least four times less sensitive to any of the four proteases.

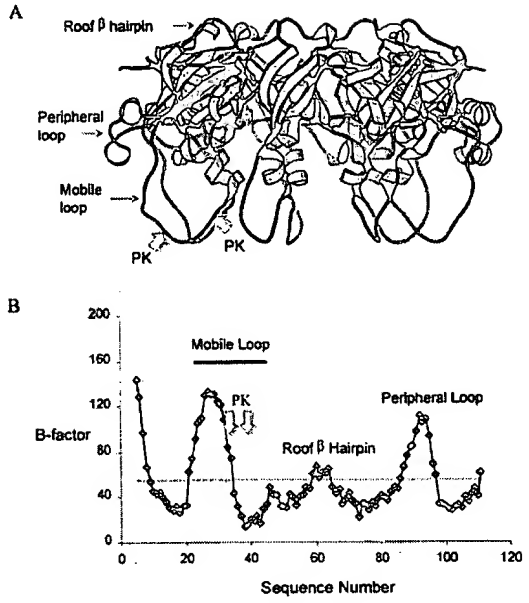

FIG. 6. **Ribbon diagram of T4Hsp10 (*A*) and plot of crystallographic B-factors for backbone amide nitrogen atoms in a single subunit of T4Hsp10 (*B*).** Preferred sites of proteolytic cleavage by protease K are illustrated. Crystallographic data were from Protein Data Bank code 1G31, and the ribbon diagram was prepared using Molscript (39). Ribbon segments corresponding to the immunodominant T-helper sequence (27) are *filled* in *black*. In *panel B*, the *horizontal dashed line* indicates the average B-factor value (55 Å), and the *horizontal bar* indicates the extent of the mobile loop defined by NMR (21). The C-terminal portion of the mobile loop, including a short α helix, mediates crystal lattice contacts with another molecule of T4Hsp10 (22); and thus B-factors do not reflect the full extent and flexibility of the mobile loop in solution. The mobile loop and two additional loops have higher than average B-factors, but only the mobile loop contains preferred cleavage sites for a variety of proteases in diverse Hsp10s. The roof β-hairpin and peripheral loop may not contain preferred cleavage sites because they are smaller and less flexible.

pin of *E. coli* Hsp10 was predicted to be metastable on the basis of its high B-factors and minimal tertiary structural contacts (36). Likewise, the roof β-hairpin of human Hsp10 has enough segmental disorder to give resolvable NMR resonances, and the roof β-hairpin was not observed in the crystal structure (37). Although highly flexible, the roof β-hairpin may be too small to accommodate the deformation required for binding to a protease. A segment of only seven residues in *E. coli* Hsp10 has B-factors that exceed the average value, and only four residues of human Hsp10 were observed by NMR. Hubbard and Thornton propose that 12 residues are necessary for efficient cleavage by trypsin (16). The peripheral loop of T4Hsp10 has 12 residues with above average B-factors, but resonances for the peripheral loop were not observed in our previous NMR study, indicating that it is not as flexible as the mobile loop. Thus, the peripheral loop is eight residues shorter than the mobile loop and much less flexible, which explains the preferential cleavage in the mobile loop.

The structure of an Hsp10 in the antigen-processing compartment should be similar to the structures previously described by x-ray crystallography and NMR. Antigen processing is believed to occur in acidic conditions in or near the lysosome. Much of the structural information about *E. coli* and human Hsp10s was gathered in acidic conditions, and the structure is essentially unchanged over a wide range of pH. Crystals of *E. coli* Hsp10 were grown at pH 5.5 (36), and NMR studies on mobile loop conformation and dynamics were carried out at pH levels ranging from 4.0 to 7.0 (23, 38). Likewise, crystals of human Hsp10 were grown at pH 3.5,[3] and NMR studies were performed from pH 3.5 to 6.8 (37). In all cases, the extent and behavior of the flexible segments were essentially identical. Thus, a highly protease-sensitive region created by local disorder in the Hsp10 structure should be the target of initial endoproteolytic cleavage *in vitro* and *in vivo*.

Three mobile loop deletion variants of T4Hsp10 were constructed to test the hypothesis that reductions in loop size and flexibility inhibit proteolytic cleavage. Low-resolution structural analysis suggests that the consequences of the deletions were restricted to the mobile loop. The behavior of the variants during purification was similar to that of T4Hsp10. The circular dichroism spectra of the variants suggest that their secondary structure content is similar to that of T4Hsp10. T4Hsp10d8C had a slightly larger β-sheet content, but this could be confined to the mobile loop. Thermal denaturation curves for the variants exhibited highly cooperative transitions, indicating that the proteins have well organized, probably native-like structure. The transition midpoints for all three variants were at elevated temperatures relative to T4Hsp10, as predicted for stabilized structure in the mobile loop. Finally, the results from chemical cross-linking suggest that the variants assume the native heptameric quaternary structure.

The mobile loop deletions reduced proteolytic sensitivity according to expected changes in loop structure and flexibility. The deletions were designed to shrink the loop and simulta-

[3] J. F. Hunt, B. J. Scott, L. Henry, J. Guidry, S. J. Landry, and J. Deisenhofer, unpublished results.

neously stabilize a nascent β-hairpin conformation. The added conformational restraints should increase the energetic cost of substrate binding to the protease. The three-residue deletion was designed to stabilize the nascent hairpin without substantially shortening the loop. Hubbard *et al.* (16) found that trypsin requires the deformation of at least 10 residues of the substrate around the cleavage site, and the deformation is much easier in a loop of 12 residues or more. Because the mobile loop of T4Hsp10 spans the 22-residue sequence from Gln^{24} to Val^{45}, removal of three residues should not severely affect the ability of the loop to be deformed. In T4Hsp10dLIG, sensitivity to protease K and cathepsin S is unaffected, and sensitivity to trypsin and protease V8 is only slightly reduced. In contrast, removal of 11 residues from the loop shrinks it to a borderline size for the deformation required by trypsin. Accordingly, T4Hsp10d8 and T4Hsp10d8C become much more resistant to trypsin and cathepsin S by comparison to T4Hsp10 and T4Hsp10dLIG.

The structure of the remaining loop segment also may influence proteolytic sensitivity. The deletion in T4Hsp10d8 leaves a segment of nascent helix intact, whereas the deletion in T4Hsp10d8C completely removes the helix. The tendency for the loop in T4Hsp10d8 (as well as T4Hsp10 and T4Hsp10dLIG) to explore alternative structures may make it more probable that the loop will adopt a conformation acceptable to the protease. In contrast, exclusive formation of β-sheet in the loop of T4Hsp10d8C would strongly disfavor proteolysis. Thus, differences in loop structure could account for the greater sensitivity of T4Hsp10d8 than T4Hsp10d8C to cleavage by proteinase K and protease V8.

The results presented here establish the broad sensitivity to proteolysis of Hsp10 mobile loops, and they support the theory that local disorder promotes presentation to helper T cells of the adjacent sequence by providing sites for proteolytic cleavage. Mobile loop deletions reduce proteolytic sensitivity to varying degrees, and the structural changes appear to be localized to the mobile loop. Thus, loop deletion provides a simple strategy for modifying epitope immunodominance.

Acknowledgments—We are grateful to P. Wittung-Stafshede and J. Guidry for access to the CD spectropolarimeter and assistance with glutaraldehyde cross-linking and to the New Orleans Protein Folding Intergroup for critical discussion.

REFERENCES

1. Janssen, R., Wauben, M., van der Zee, R., de Gast, M., and Tommassen, J. (1994) *Int. Immunol.* **6,** 1187–1193
2. Ma, C., Whiteley, P. E., Cameron, P. M., Freed, D. C., Pressey, A., Chen, S. L., Garni-Wagner, B., Fang, C., Zaller, D. M., Wicker, L. S., and Blum, J. S. (1999) *J. Immunol.* **163,** 6413–6423
3. Chianese-Bullock, K. A., Russell, H. I., Moller, C., Gerhard, W., Monaco, J. J., and Eisenlohr, L. C. (1998) *J. Immunol.* **161,** 1599–1607
4. Vanegas, R. A., Street, N. E., and Joys, T. M. (1997) *Vaccine* **15,** 321–324
5. Manca, F., Fenoglio, D., Valle, M. T., Li, P. G., Kunkl, A., Ferraris, A., Saverino, D., Lancia, F., Mortara, L., Lozzi, L., Pierres, M., Dalgleish, A., and Lewis, G. (1995) *J. Acquired Immune Defic. Syndr. Hum. Retrovirol.* **9,** 227–237
6. Phelps, R. G., Jones, V. L., Coughlan, M., Turner, A. N., and Rees, A. J. (1998) *J. Biol. Chem.* **273,** 11440–11447
7. Moudgil, K. D., Deng, H., Nanda, N. K., Grewal, I. S., Ametani, A., and Sercarz, E. E. (1996) *J. Autoimmun.* **9,** 227–234
8. Castellino, F., Zappacosta, F., Coligan, J. E., and Germain, R. N. (1998) *J. Immunol.* **161,** 4048–4057
9. Nakagawa, T. Y., and Rudensky, A. Y. (1999) *Immunol. Rev.* **172,** 121–129
10. Van Noort, J. M., Boon, J., Van der Drift, A. C. M., Wagenaar, J. P. A., Boots, A. M. H., and Boog, C. J. P. (1991) *Eur. J. Immunol.* **21,** 1989–1996
11. Schneider, S. C., Ohmen, J., Fosdick, L., Gladstone, B., Guo, J., Ametani, A., Sercarz, E. E., and Deng, H. (2000) *J. Immunol.* **165,** 20–23
12. Antoniou, A. N., Blackwood, S. L., Mazzeo, D., and Watts, C. (2000) *Immunity* **12,** 391–398
13. So, T., Ito, H., Koga, T., Watanabe, S., Ueda, T., and Imoto, T. (1997) *J. Biol. Chem.* **272,** 32136–32140
14. Novotny, J., and Bruccoleri, R. E. (1987) *FEBS Lett.* **211,** 185–189
15. Hubbard, S. J., Campbell, S. F., and Thornton, J. M. (1991) *J. Mol. Biol.* **220,** 507–530
16. Hubbard, S. J., Eisenmenger, F., and Thornton, J. M. (1994) *Protein Sci.* **3,** 757–768
17. Drakesmith, H., ONeil, D., Schneider, S. C., Binks, M., Medd, P., Sercarz, E., Beverley, P., and Chain, B. (1998) *Proc. Natl. Acad. Sci. U. S. A.* **95,** 14903–14908
18. Dill, K. A., and Shortle, D. (1991) *Annu. Rev. Biochem.* **60,** 795–825
19. Landry, S. J. (1997) *Immunol. Today* **18,** 527–532
20. Landry, S. J. (2000) *J. Theor. Biol.* **203,** 189–201
21. Landry, S. J., Taher, A., Georgopoulos, C., and van der Vies, S. *M. (1996) Proc. Natl. Acad. Sci. U. S. A.* **93,** 11622–11627
22. Hunt, J. F., van der Vies, S. M., Henry, L., and Deisenhofer, J. (1997) *Cell* **90,** 361–371
23. Landry, S. J., Zeilstra-Ryalls, J., Fayet, O., Georgopoulos, C., and Gierasch, L. M. (1993) *Nature* **364,** 255–258
24. Kim, J., Sette, A., Rodda, S., Southwood, S., Sieling, P. A., Mehra, V., Ohmen, J. D., Oliveros, J., Appella, E., Higashimoto, Y., Rea, T. H., Bloom, B. R., and Modlin, R. L. (1997) *J. Immunol.* **159,** 335–343
25. Hussain, R., Dockrell, H. M., Shahid, F., Zafar, S., and Chiang, T. J. (1998) *Clin. Exp. Immunol.* **114,** 204–209
26. Chualntra, B., Ivanyi, J., Hills, A., Thole, J., Moreno, C., and Vordermeier, H. M. (1998) *Immunology* **93,** 64–72
27. Dai, G., Carmicle, S., Steede, N. K., and Landry, S. J. (2002) *J. Biol. Chem.* **277,** 161–168
28. van der Vies, S. M., Gatenby, A. A., and Georgopoulos, C. (1994) *Nature* **368,** 654–656
29. Schagger, H., and von Jagow, G. (1987) *Anal. Biochem.* **166,** 368–379
30. Pace, C. N., Hebert, E. J., Shaw, K. L., Schell, D., Both, V., Krajcikova, D., Sevcik, J., Wilson, K. S., Dauter, Z., Hartley, R. W., and Grimsley, G. R. (1998) *J. Mol. Biol.* **279,** 271–286
31. Richardson, A., vanderVies, S. M., Keppel, F., Taher, A., Landry, S. J., and Georgopoulos, C. (1999) *J. Biol. Chem.* **274,** 52–58
32. Brahms, S., Brahms, J., Spach, G., and Brack, A. (1977) *Proc. Natl. Acad. Sci. U. S. A.* **74,** 3208–3212
33. Benaroudj, N., Fang, B., Triniolles, F., Ghelis, C., and Ladjimi, M. M. (1994) *Eur. J. Biochem.* **221,** 121–128
34. Farr, C. D., Slepenkov, S. V., and Witt, S. N. (1998) *J. Biol. Chem.* **273,** 9744–9748
35. Barrett, A. J., Rawlings, N. D., and Woessner, J. F. (eds) (1998) *Handbook of Proteolytic Enzymes,* Academic Press, San Diego
36. Hunt, J. F., Weaver, A. J., Landry, S. J., Gierasch, L. M., and Deisenhofer, J. (1996) *Nature* **379,** 37–45
37. Landry, S. J., Steede, N. K., and Maskos, K. (1997) *Biochemistry* **36,** 10975–10986
38. Landry, S. J., Steede, N. K., Garaudy, A. M., Maskos, K., and Viitanen, P. V. (1999) in *Pacific Symposium on Biocomputing '99* (Altman, R. B., Dunker, A. K., Hunter, L., Klein, T. E., and Lauderdale, K., eds) pp. 520–531, World Scientific, Singapore
39. Kraulis, P. J. (1991) *J. Appl. Crystallogr.* **24,** 946–950